and serum level of gonadotropin were normal. Light and scanning electron microscopy of her hair demonstrated classical findings of pili torti with hair shafts being flattened at irregular intervals and twisted 180 degrees from the normal axis (Fig. 1d,e) and with partial trichorrhexis (Fig. 1f). After obtaining informed consent, genomic DNA was obtained from peripheral blood samples of the patient, her parents and control individuals using a NucleoSpin Blood QuickPure kit (TaKaRa, Otsu, Japan) according to the manufacturer's instructions. All seven exons and exon–intron boundaries of *BCS1L* (accession number AF346835.1) were amplified by polymerase chain reaction (PCR) using gene-specific primers and PCR conditions as described previously.[4] The amplified PCR products were purified and directly sequenced. DNA sequencing and mutation analysis revealed compound heterozygous mutations of c.916C>T transition and c.1201_1202insA in the patient (Fig. 2a). Heterozygous transition C>T at nucleotide position 916 in exon 6 of the *BCS1L* gene caused the missense mutation p.R306C, while a heterozygous insertion of A between nucleotide positions 1201 and 1202 in exon 7 of the *BCS1L* gene, which resulted in a frameshift, led to a deletion of 49 bp (16 amino acids) and a premature termination codon at four amino acid residues downstream of the mutation (p.M401NfsX4) (Fig. 2a,c). The mutations of c.916C>T and c.1201_1202insA were inherited from the father and mother, respectively, and both mutations were absent in 106 unrelated Japanese healthy control individuals (Fig. 2a–d). A diagnosis of Björnstad syndrome was made on the basis of these clinical findings and results of DNA mutation analysis.

In 1965, Björnstad first described the combination of pili torti and sensorineural deafness as a novel genetic entity.[1] Usual clinical features are pili torti and sensorineural deafness.[4] Other accompanying symptoms such as atrophic testis, micropenis and mental retardation have been reported,[5] but their frequencies are unknown. Our case showed classical pili torti and trichorrhexis caused by spontaneous breakage of twisted hairs. Hair diseases with pili torti, including Menkes disease, ectodermal dysplasia and Crandall syndrome, are considered as differential diagnoses. Crandall syndrome includes pili torti and sensorineural deafness with the additional finding of hypogonadism.[6] Menkes kinky hair disease is an X-linked recessive disorder of copper metabolism diagnosed by a low plasma level of copper.[7] Ectodermal dysplasia is characterized by deformity of hair, teeth, nails and sweat glands.[7] Because no additional abnormalities were found in our case, these differential diagnoses could be ruled out.

Björnstad syndrome has been diagnosed only by clinical symptoms including pili torti and sensorineural deafness. In 1998, it was shown that the locus responsible for the syndrome is mapped to chromosome 2q34–36.[8] In 2007, Hinson *et al.*[9] identified a missense mutation in the *BCS1L* gene as a cause of Björnstad syndrome (Fig. 2e). Mutations in the *BCS1L* gene were previously shown to cause mitochondrial complex III deficiency (OMIM 124000), manifested by neonatal renal tubulopathy, encephalopathy and liver failure, and GRACILE syndrome (OMIM 603358)[4] with a severe type of mitochondrial complex III deficiency. These two syndromes are fatal diseases and do not show hair abnormalities. BCS1L, a 419-amino-acid chaperone protein, is a member of the family called AAA, an acronym for ATPases associated with various cellular activities.[9] All *BCS1L* mutations increase the production of reactive oxygen species (ROS), and the increased ROS production causes clinical symptoms.[9] Mutations associated with mitochondrial complex III deficiency and GRACILE syndrome were shown to be located at sites of direct interaction with magnesium or ATP on the three-dimensional structure of RuvB, which has the highest sequence homology to BCS1L of all AAA domains.[9] In contrast, mutations caused by Björnstad syndrome are located on the exterior face of the AAA domain.[9] In fact, the mutations of p.R306C and p.M401NfsX4 in our case were located on the exterior face of the AAA domain (Fig. 2f). A wide range of clinical phenotypes seem to be caused by different amounts of increased ROS production due to BCS1L functional inhibition depending on the location of *BCS1L* gene mutations.

We identified a novel *BCS1L* gene mutation with compound heterozygosity for missense and nonsense mutations by a frameshift. Both mutations are predicted to be recessive mutations that would not show a dominant negative effect, as the parents, who each had one of the mutations heterozygously, exhibited a normal hair phenotype. The arginine residue at codon 306, which was converted to cysteine by c.916C>T, is conserved among *BCS1L* in diverse species (Fig. 2g). Because the cysteine is covalently bonded to other cysteine residues to form disulfide bonds, the BCS1L protein structure would be affected by the mutation. In addition, the frameshift mutation in exon 7 is predicted to result in a premature termination codon and the mutant *BCS1L* transcripts would be degraded by nonsense-mediated mRNA decay, although the position of the mutation in exon 7 is not a main functional domain (Fig. 2e,f). We speculated that Björnstad syndrome developed due to inhibition of BCS1L protein function from these compound heterozygous mutations in our case. Future functional studies may verify the pathogenicity of these mutations.

[1]*Department of Dermatology, Aichi Medical University School of Medicine, Nagakute, Aichi 480-1195, Japan*
[2]*Department of Dermatology, Nagoya University Graduate School of Medicine, 65 Tsurumai-cho, Showa-ku, Nagoya 466-8500, Japan*
[3]*Department of Biomedical Sciences, College of Life and Health Sciences, Chubu University, Kasugai, Aichi 487-8501, Japan*
E-mail: takeshit@aichi-med-u.ac.jp

T. YANAGISHITA[1]
K. SUGIURA[2]
Y. KAWAMOTO[3]
K. ITO[1]
Y. MARUBASHI[1]
N. TAGUCHI[1]
M. AKIYAMA[2]
D. WATANABE[1]

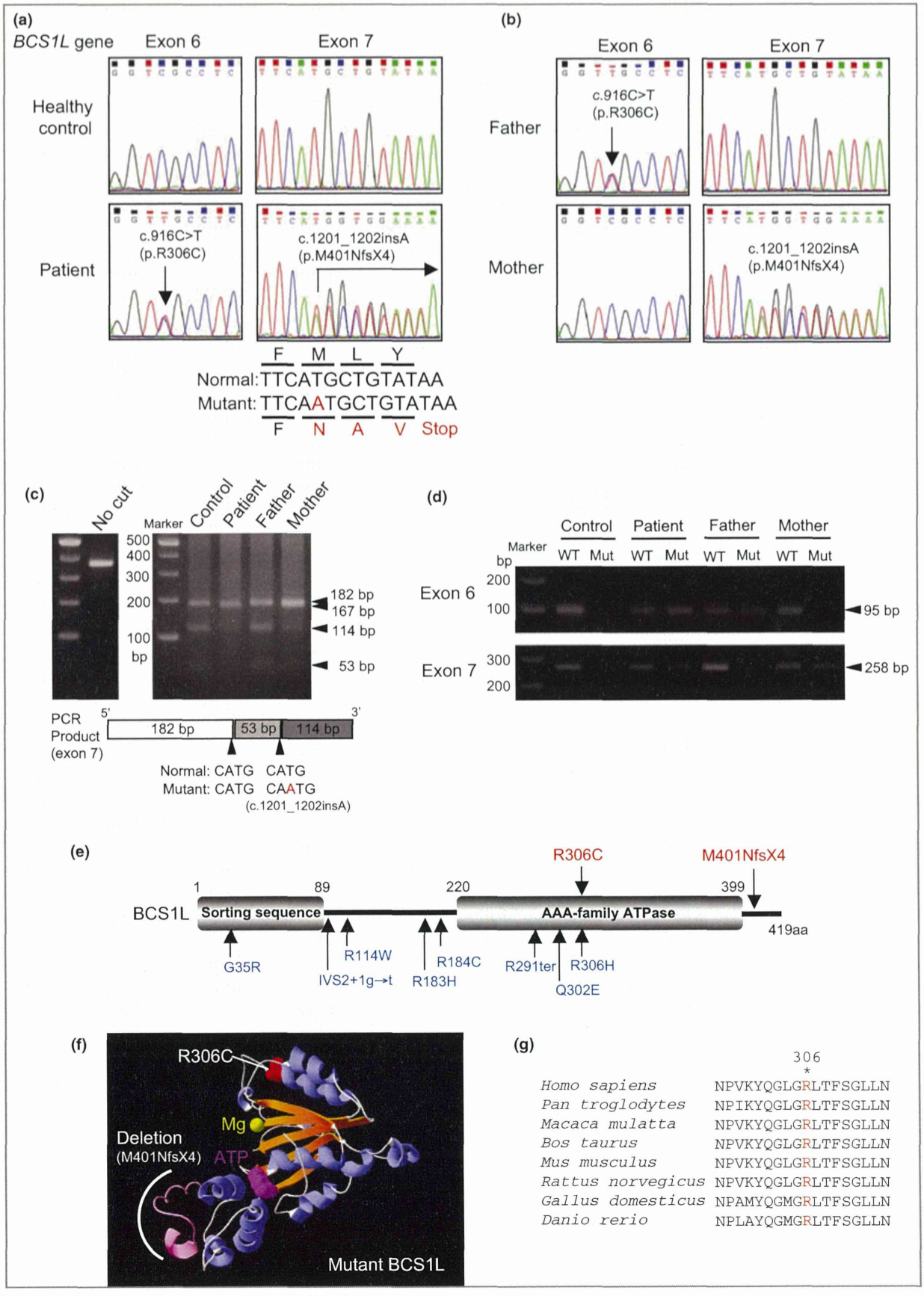

Fig 2. Identification of compound heterozygous mutations in the *BCS1L* gene. (a) The heterozygous mutation c.916C>T (p.R306C) was identified in exon 6 of *BCS1L*. The position of the transition is indicated by an arrow. The heterozygous mutation c.1201_1202insA (p.M401NfsX4) was identified in exon 7 of *BCS1L*. Both mutations were absent in healthy control individuals. (b) The mutations of c.916C>T (p.R306C) and c.1201_1202insA (p.M401NfsX4) were inherited from the father and mother, respectively. (c) PCR-RFLP assay for the mutation c.1201_1202insA in exon 7. The PCR products were digested by *Nla*III restriction enzyme. The c.1201_1202insA heterozygous mutation was inherited from the unaffected mother. Details are shown in the Supplementary information. (d) Data of the mutant allele-specific PCR amplication. The primer sequences and PCR conditions are shown in the Supplementary information. (c) 916C>T heterozygous mutation in exon 6 exists in the patient's and father's *BCS1L* gene. The c.1201_1202insA heterozygous mutation in exon 7 exists in the patient's and mother's *BCS1L* gene. (e) Schema of BCS1L protein with the mitochondrial sorting sequence domain (residues 1–89) and the conserved AAA-family ATPase domain (residues 220–399). Homozygous mutations identified to date are shown in blue. The mutations identified in our case are shown in red. (f) Theoretical ribbon structures of the AAA domains from partial *BCS1L* show locations of the p.R306C mutation (red) and p.M401NfsX4 mutation (pink) relative to magnesium (yellow) and ATP (purple). Details are shown in the Supplementary information. (g) The arginine residue at codon 306, which was converted to cysteine, is conserved among *BCS1L* in diverse species. PCR-RFLP, polymerase chain reaction–restriction fragment length polymorphism.

References

1 Selvaag E. Pili torti and sensorineural hearing loss. A follow-up of Bjørnstad's original patients and a review of the literature. *Eur J Dermatol* 2000; **10**:91–7.

2 Aggarwal D, Sardana K, Kumar P *et al.* Björnstad syndrome. *Indian J Pediatr* 2004; **71**:759–61.

3 Richards KA, Mancini AJ. Three members of a family with pili torti and sensorineural hearing loss: the Bjornstad syndrome. *J Am Acad Dermatol* 2002; **46**:301–3.

4 de Lonlay P, Valnot I, Barrientos A *et al.* A mutant mitochondrial respiratory chain assembly protein causes complex III deficiency in patients with tubulopathy, encephalopathy and liver failure. *Nat Genet* 2001; **29**:57–60.

5 Loche F, Bayle-Lebey P, Carriere JP *et al.* Pili torti with congenital deafness (Bjornstad syndrome): a case report. *Pediatr Dermatol* 1999; **16**:220–1.

6 Crandall BF, Samec L, Sparkes RS *et al.* A familial syndrome of deafness, alopecia, and hypogonadism. *J Pediatr* 1973; **82**:461–5.

7 Silengo M, Valenzise M, Sorasio L *et al.* Hair as a diagnostic tool in dysmorphology. *Clin Genet* 2002; **62**:270–2.

8 Lubianca Neto JF, Lu L, Eavey RD *et al.* The Bjornstad syndrome (sensorineural hearing loss and pili torti) disease gene maps to chromosome 2q34–36. *Am J Hum Genet* 1998; **62**:1107–12.

9 Hinson JT, Fantin VR, Schönberger J *et al.* Missense mutations in the BCS 1L gene as a cause of the Björnstad syndrome. *N Engl J Med* 2007; **356**:809–19.

Supporting Information

Additional Supporting Information may be found in the online version of this article at the publisher's website:

Supplementary information relating to Figure 2c in the main text. PCR-RFLP assay for the mutation in exon 7. PCR products from the control and the father were digested to 182-bp, 114-bp and 53-bp fragments, whereas PCR products from the patient and the mother were digested to 182-bp homogeneously and 167-bp (undivided to a 182-bp band), 114-bp and 53-bp fragments heterogeneously by *Nla*III restriction enzyme at 37 °C for 1 h and run on 3% agarose gel. The c.1201_1202insA heterozygous mutation was inherited from the unaffected mother. The wild type or mutation c.916C>T in exon 6 did not create or destroy a restriction enzyme site. PCR-RFLP, polymerase chain reaction -restriction fragment length polymorphism.

Supplementary information relating to Figure 2d in the main text. Sequences of primers and PCR conditions for mutant allele-specific PCR. Primer sequences (exon 6) were 5′-TCCACTGAAGGTGAGGCG-3′ (reverse) for the wild-type allele, 5′-TCCACTGAAGGTGAGGCA-3′ (reverse) for the mutant allele (3′ end mismatched) and 5′-TTTATGCTGGGCTATGACTACT-3′ (forward) for the common allele. The PCR product size was 95 bp. Primer sequences (exon 7) were 5′-CAGGGTCATTTTTATACAGCATG-3′ (reverse) for the wild-type allele, 5′-CAGGGTCATTTTTATACAGCATT-3′ (reverse) for the mutant allele and 5′-TGGGTGCTAGTGTGACCTGC-3′ (forward) for the common allele in exon 7. The PCR product size was 258 bp. PCR conditions were 94 °C for 2 min, followed by 35 cycles of 94 °C for 15 s, 60 °C for 30 s and 68 °C for 30 s, with a final extension step at 68 °C for 7 min. PCR products were electrophoresed in 3% agarose gels and visualized by GelRed™ (WAKO, Osaka, Japan) staining.

Supplementary information relating to Figure 2f in the main text. Locations of mutations in our case on three-dimensional structures of *BCS1L*. Theoretical ribbon structures of the AAA domains from partial BCS1L analysed by the SWISS-MODEL homology modelling show locations of the p.R306C mutation (red) and p.M401NfsX4 mutation (pink) relative to magnesium (yellow) and ATP (purple). The residues 401–419 (deletion part: p.M401NfsX4) could not be matched by homology modelling. Therefore, only these sequences were matched with RuvB, which has the highest sequence homology to BCS1L and AAA family, and merged with *BCS1L* structures.

Funding sources: No external funding.

Conflicts of interest: None declared.

All study participants provided informed consent.